Article:
Velasquez, SM, Marzol, E, Borassi, C et al. (2015) Low Sugar Is Not Always Good: Impact of Specific O-Glycan Defects on Tip Growth in Arabidopsis. Plant Physiology, 168 (3). pp. 808-813. ISSN: 0032-0889

https://doi.org/10.1104/pp.114.255521

Plant Physiology Preview. Published on May 5, 2015, as DOI:10.1104/pp.114.255521

Scientific Correspondence

Low sugar is not always good: Impact of specific *O*-glycan defects on tip growth in *Arabidopsis*

Silvia M. Velasquez[1], Eliana Marzol[1], Cecilia Borassi[1], Laercio Pol-Fachin[2,3], Martiniano M. Ricardi[1], Silvina Mangano[1], Silvina Paola Denita Juarez[1], Juan D. Salgado Salter[1], Javier Gloazzo Dorosz[1], Susan E. Marcus[4], J. Paul Knox[4], Jose R. Dinneny[5], Norberto D. Iusem[1,6], Hugo Verli[3] & José M. Estevez[1,†]

[1]Instituto de Fisiología, Biología Molecular y Neurociencias (IFIBYNE-CONICET), Facultad de Ciencias Exactas y Naturales, Universidad de Buenos Aires C1428EGA, Argentina.
[2]Departamento de Química Fundamental, Universidade Federal de Pernambuco, Brasil.
[3]Centro de Biotecnologia, Universidade Federal do Rio Grande do Sul, Brasil.
[4]Centre for Plant Sciences, Faculty of Biological Sciences, University of Leeds, Leeds LS2 9JT, UK.
[5]Carnegie Institution for Science, Department of Plant Biology, Stanford, California 94305.
[6]Departamento de Fisiología, Biología Molecular y Celular. Laboratorio de Fisiología y Biología Molecular (LFBM), Facultad de Ciencias Exactas y Naturales, Universidad de Buenos Aires, Buenos Aires C1428EGA, Argentina.

[†] Correspondence should be addressed. Email: jestevez@fbmc.fcen.uba.ar

Hydroxyproline-rich *O*-glycoproteins (HRGPs) comprises several groups of *O*-glycoproteins including extensins (EXTs), ultimately secreted into plant cell walls. The latter are shaped by several posttranslational modifications (PTMs), mainly hydroxylation of proline residues into hydroxyproline (Hyp) and further *O*-glycosylation on Hyp and Serine (Ser) (**Fig. S1A**). EXTs contain several Ser-$(Hyp)_4$ repeats usually *O*-glycosylated with chains of up to 4-5 linear arabinosyl units (Ara) on each Hyp (Velasquez et al., 2011; Ogawa-Ohnishi et al., 2013) and mono-galactosylated on Ser residues (Saito et al., 2014). *O*-glycosylated Ser-$(Hyp)_4$ repeats are not only present in EXTs but they can potentially be decorating several other EXT-like chimeras and hybrid-EXT glycoproteins that contain other domains such as AGP (ArabinoGalactan Protein)-EXTs, Proline Rich Proteins (PRP)-EXTs, Leucine Rich Repeats (LRR)-EXTs, Proline-Rich Kinases (PERKs) and Formins with an extracellular EXTs domain, etc. In addition, Hyp-*O*-arabinosylation also occurs in single Hyp units in the small secreted glycopeptide hormones (e.g. CLAVATA 3, CLV3) with up to 3 Ara units (Ohyama et al., 2009; Matsubayashi, 2010; Shinohara and Matsubayashi, 2013). In this context, three groups of arabinosyltransferases (AraTs), HPAT1-HPAT3 (classified as GT8 in the Carbohydrate Active enZymes database [CAZy]), RRA1-RRA3 and XEG113 (GT77 family) have recently been implicated in the sequential addition of the innermost three L-Ara residues (Egelund et al., 2007; Ogawa-Ohnishi et al., 2013) (**Table S1**). In addition, one novel peptidyl-Ser galactosyltransferase named SERGT1 has been reported to add a single α-Gal*p* (Galactopyranose) residue to each Ser residue in Ser-$(Hyp)_4$ motifs of EXTs, thus belonging to GT96 family within CAZy (**Table S1**). Finally, glycosylated EXTs are possibly crosslinked by putative type-III peroxidases (PERs) at the Tyr residues forming EXT linkages (Cannon et al., 2008) able to build a three-dimensional network likely to interact with other cell wall components like pectins (Cannon et al., 2008). EXT assembly into a putative glycoprotein network seems to be crucial for cell expansion of root hairs and several EXT and EXT-related mutants (e.g. *ext6-7*, *ext10-12*, *lrx1*, etc.) were previously isolated with abnormal root hair cell expansion phenotypes (Ringli, 2010; Velasquez et al., 2011). Here, by using mutants of several known enzymes of the *O*-glycosylation pathway of HRGPs, we addressed to what extent each specific defect on the *O*-glycosylation machinery impacts on root hair tip growth. In addition,

we refer only to Hyp-*O*-arabinosylation and Ser-*O*-galactosylation modifications of EXT and EXT-related proteins while we have excluded Hyp *O*-(arabino)galactosylation, commonly present in other type of HRGP like AGPs, from our analysis. Finally, by molecular dynamic simulations, we propose a possible model to explore how these two specific types of *O*-glycan defects would affect EXT self-assembly and, ultimately, their impact on the polarized cell expansion. We use a classical EXT repetitive sequence to begin to explore how *O*-glycosylation might affect glycoprotein conformation and possible self-interactions in the context of polarized growth but we are aware of the complexity and diversity of EXT and EXT-related proteins that offers several other possible scenarios.

***O*-Glycosylation changes in HRGPs have an impact on root hair tip-growth.** The currently known enzymes that define Hyp-*O*-arabinosylation in EXTs and related HRGPs are P4H5,2,13 and RRA3-XEG113 as well as HPAT1-HPAT3 (**Table S1**). All these arabinosyltrasnferases (AraTs) are highly expressed specifically in root hair cells (**Fig. 1A**) and also co-regulated systemically at the transcriptional level together with prolyl 4-hydroxylases 2 (P4H2) and P4H5 (**Fig. 1B**). This suggested that all these enzymes required to *O*-glycosylate EXTs and related glycoproteins are particularly relevant for root hair growth. Consequently, we analyzed insertional T-DNA mutants for HPAT1-3 enzymes (single mutant *hpat1-hpat3* as well as the double *hpat1 hpat2*), which add the first arabinose onto Hyp units in EXTs and EXT-related proteins as well as in secreted small peptides (Ogawa-Ohnishi et al., 2013). *hpat1-hpat3* available mutants were reported to lack the corresponding HPAT1-3 transcripts. We found that they displayed a short root hair phenotype in accordance with the other two previously described AraT mutants, *rra3* and *xeg113* (**Fig. 1C**) (Egelund et al., 2007; Gille et al., 2009). In addition, *hpat* mutants displayed longer hypocotyls (*hpat1,hpat2*) and shorter pollen tubes (*hpat1/+,hpat2/+*) (Ogawa-Ohnishi et al., 2013). By using a genome-wide expression analysis and reverse genetics, we identified a gene, At3g01720, which is highly co-expressed with P4H2-P4H5 as well as with HPAT3, RRA3, and XEG113 (**Fig. 1B**) in root hair cells (**Fig. 1A**). Recently, it was shown that At3g01720, originally named as SGT1 (here as we will refer as

SERGT1 since several other proteins already contain SGT1 acronym), encodes a protein with *in vitro* Ser α-galactosyltransferase activity on a short EXT-like peptide substrate (**Fig. S1A**) (Saito et al., 2014), although no involvement in root hair growth was reported then. Therefore, we analyzed two null homozygous T-DNA mutants available for At3g01720, *sergt1-1* and *sergt1-2*, both of which displayed a drastic reduction in root hair length (**Fig. 1C-D**) similar to that found in the previously characterized Ara*T*s insertional mutants *rra3* and *xeg113*-2 (**Fig. 1C)** (Velasquez et al., 2011). These results together support the idea that the single *O*-galactosylation event performed by SERGT1 is also required for EXT (and EXT-related proteins)-mediated root hair tip growth. In addition, *sergt1-1* and *sergt1-2* mutants showed additional plant developmental phenotypes such as longer roots and larger leaves, indicating that SERGT1 is also relevant for the cell expansion process in other cell types (Saito et al., 2014).

Enhanced effects of two different *O*-glycan deficiencies on root hair tip growth. Next, we investigated the physiological contributions to tip growth of both *O*-arabinosylation and single *O*-galactosylation deficiencies on the HRGPs and related proteins. To block P4H activity in the *sgt1-1* mutant root hairs (**Fig. 1E-F**), we treated roots with the P4H inhibitors EDHB (ethyl-3,4-dihydroxybenzoate), which interacts with the active oxoglutarate binding site of P4Hs and DP (α,α-dipyridyl), which chelates the cofactor Fe^{2+}. Previously to this work, the inhibitory concentration 50 (IC_{50}) was determined for both inhibitors, EDHB (219 nM) and DP (48 nM) (Velasquez et al., 2011). Being aware of the risk of disturbing other targets and having undesirable consequences on growth when using pharmacological inhibitors like EDHB and DP to inhibit P4H activity, we also followed a genetic approach. Consistently, the growth inhibitory effect observed with either compound was in the same range as the one in the *p4h5* and *p4h2,5,13* mutants (Velasquez et al., 2011; Velasquez et al., 2014). Both P4H inhibitors (DP and EDHB at IC_{50} doses) led to further root hair growth impairment in *sergt1-1* compared to non-treated *sergt1-1*. Then, we tested the effect on root hair growth in *p4h5* and *sergt1-1* as well as *p4h5 sergt1-1* and *rra3 sergt1-1* double mutants (**Fig. 1G-H**). The

combined and simultaneous deficiencies of both *O*-glycan types showed an increased inhibitory effect on tip growth when compared with the impairment displayed by the corresponding single mutants. These results together suggest that the two types of *O*-glycosylation, Hyp-*O*-arabinosylation and Ser-*O*-galactosylation, are central for the functionality of EXTs and EXT-related proteins. Also, the combined deficiency of both glycan types has a strong inhibitory effect on root hair tip growth. It is important to emphasize that the status of *O*-glycosylation, including Hyp-*O*-arabinosylation and Ser-*O*-Galactosylation, in several related HRGP-proteins other than EXTs and in small secreted glycopeptides (e.g. CLV3) would be also possibly affected in the AraT described mutants (**Table S1**) and these changes could also contribute to the root hair phenotype reported here. However, as highlighted before, several EXT and EXT-related mutants were previously reported to have short and abnormal root hair phenotypes (Ringli, 2010; Velasquez et al., 2011) suggesting a major role of the EXT proteins in root hair cell expansion.

To understand how *O*-glycosylation defects in EXTs and EXT-related proteins modify the temporal dynamics of polarized cell expansion, we measured two key variables in tip growth: the growth rate and the active growth time over a 4 hour period. Most of the deficient *O*-glycosylation mutants tested (*p4h5*, *xeg113-2*, *sergt1-1* and *p4h5 sergt1*) showed a drastically lower growth rate as well as a much shorter final time than Wt (**Fig. 1I**; **Fig. S2**), confirming that shorter root hairs are a consequence of both a drastically reduced growth rate and premature cessation of growth. On the other hand, the resulting phenotype of extra-long root hairs in the overexpressing $35S_{pro}$::P4H5 line (in Wt background; **Fig. 1I**) is explained exclusively on a higher growth rate but with a similar active growth time (**Fig. S2**). This clearly confirms that the *O*-glycosylation status of EXTs and related EXT-proteins impacts on the temporal dynamics of tip growth.

To confirm that changes in the *O*-glycosylated EXTs and EXT-related proteins are located to the actively growing root hair cell walls, an *in situ* immunolabeling assay was performed using a monoclonal antibody (JIM20) that specifically recognizes *O*-glycans in EXTs (Smallwood et al.,

1994) (**Fig. 1J**). In root hairs of the *rra3* mutant, in which there is only one arabinosyl unit instead of the 4 arabinosyl units usually found in Wt root EXTs (Velasquez et al., 2011) no signal was detected. The JIM20 signal was lower in *p4h5* compared to Wt but still higher than in *rra3* root hairs (**Fig. 1J**), proving that the few Hyp residues in EXTs from *p4h5* still carry full *O*-arabinoside chains. On the other hand, root hairs in the $35S_{pro}$::P4H5/Wt overexpresor line showed stronger JIM20 labelling than Wt. This implies that not all proline units in EXTs and related proteins normally present in root hair cells are fully hydroxylated by P4Hs. In addition, at least for EXT3, around 20% of Hyp units are in the non-glycosylated form (Cannon et al., 2008). In synthetic peptides with EXT motifs expressed in tobacco BY2 cells, 5-8% were also in the non-glycosyltased Hyp form (Shpak et al., 2001; Held et al., 2004), leaving the question of how this process is regulated at the molecular level. Finally, cell walls in *sergt1-1* showed normal labelling, revealing that, despite the clear hair growth phenotype observed, the lack of serine-*O*-galactosylation does not affect Hyp-*O*-arabinosylation.

Differential *O*-glycosylation on an EXT sequence influences its protein conformation. To understand the effects of differential *O*-glycosylation on an EXT sequence, structure and conformation, and its relation to root hair tip growth, we performed molecular dynamics (MD) simulations on four EXT repeating unit glycoforms: non-glycosylated, *O*-galactosylated, *O*-arabinosylated and Wt *O*-glycosylated EXTs. From such simulations, the Wt glycosylated EXT peptide is observed to present the less extended structure (**Fig. S3A**, blue structure), showing curvatures around the SPPPP moiety (where S=Serine and P=Proline). Also, the degree of peptide extension progressively increases in an inversely proportional matter to glycosylation content, being almost fully extended in non-glycosylated EXT peptide (**Fig. S3A**, black structure). Considering the lower root hair tip growth rate in the mutant lines containing possibly a higher fraction of low or non-glycosylated EXTs and EXT-related proteins, Wt *O*-glycosylation may be related to a correct EXT "folding", thus required for a proper root hair tip growth. Based on our simulations, we can predict that Wt *O*-glycosylated EXT molecule maintains Tyr8:OH and Tyr6:Cε2 atoms in close proximity (0.75 ± 0.22 nm) compared to a non-glycosylated (1.02 ± 0.41 nm) form and intermediate in the single *O*-galactosylated (0.93

± 0.39 nm) EXT systems (**Fig. S3B**), thus possibly facilitating the formation of isodityrosine (IDT) from alternating Tyr residues on YVY motifs. Hence, correct Hyp-*O*-arabinosylation appears to be responsible for generating a bend on EXT backbone around a YVY motif (**Fig. S3A**, green and blue structures), which may represent a better scenario for Tyr intra-molecular EXT-crosslinks (IDT type). Such bend promoted by Hyp-*O*-arabinosylation also appears to form a framework to expose such Tyr residues to solvent and, consequently, inter-molecular EXT Tyr-crosslink linkages formation mechanisms. It is possible that abnormal or absence of *O*-glycosylation on EXT molecules would trigger other changes not included in this analysis (e.g. affect the putative EXT interaction with other cell wall polymers like pectin as it suggested before (Nuñez et al., 2009; Valentin et al., 2010)).

A highly branched and dendritic EXT network with up to six putative overlapped monomeric chains for each segment (with 127 nm in average length) was previously visualized by Atomic Force Microscopy in a *in vitro* system with purified EXT3 monomers from *Arabidopsis* cell culture (Cannon et al., 2008). The three-dimensional EXT network could self-assemble by a proposed staggered lateral alignment mechanism and Tyr-*intra* and *inter*-molecular crosslinkings, including isodityrosine, pulcherosine and di-isodityrosine covalent linkages (**Fig. 2A**) (Cannon et al., 2008). While several possible supramolecular assemblies were explored by MD simulations for individual EXT chains, including dimers, trimers and tetramers, the trimeric collagen triple helix was the more favorable one due to its conformational compactness, that is, the closer proximity between its composing chains. However, considering the possible influence of other cell wall components, as cellulose, pectins and other structural proteins, over EXT assembly, the putative trimeric organization may not be the only one observed physiologically. Nevertheless, non-glycosylated EXT monomeric chains could be assembled in a triple helix with similar interaction energies (-1423 +-93 kJ/mol) comparable to the collagen macromolecular structure (-1317 +-37 kJ/mol) (**Fig. 2C-D**), whereas the glycosylated EXT state (with -1093 +-48 kJ/mol) deviates to a less stable and more chaotic assemblage of the triple chain structure (**Fig. 2B-E**). This suggests that PMTs of individual EXT chains would have a strong impact on their assemblage properties at the cell

wall. Specifically, we propose that high levels of *O*-glycosylation in certain EXT segments will impose a physical restriction to EXTs lateral alignments, probably acting as a twist or branching point, which would favour the development of a putative more relaxed cell wall network. Though there is no evolutionary homology between collagen and EXT proteins, they could represent a case of structural convergence in extracellular matrix environments. Further experiments are needed to confirm if EXT sequences are able to form stable *in vitro* triple helix assemblages, and then, if these suprastructures can be detected *in situ* in the plant cell walls.

Why are these extracellular EXT assemblies biologically relevant?. Previously, it has been suggested that the *O*-glycans present in the single polyproline type-II helix, like those present in EXTs, would provide conformational and thermal stability to these macromolecules by enhancing inter-glycan and glycan-peptide hydrogen bonding (Owens et al., 2010). In accordance, the biological activity of the glycopeptide hormone CLV3 in stem cell fate is also progressively enhanced with increasing arabinose chain length with up to three arabinose with β-1,2 bonds on Hyp units (Shinohara and Matsubayashi, 2013) with a chemistry identical to that of EXTs and related *O*-glycoproteins (**Fig. S1B**). Recently, a complete stereo-selective synthesis of a fully glycosylated Ser-Hyp pentapeptide motif was achieved, confirming a polyproline left-handed helix-like structure as proposed for endogenous EXTs (Ishiwata et al., 2014). In particular, we propose that the *O*-glycan-promoted loose conformation of the helical assembly favours root hair growth. Consistently, this model predicts a non-glycosylated EXT helix as a rigid structure that impairs cell expansion. These spatial alterations are likely to be mediated by Tyr-Tyr linkages during assembly into the cell wall, with a noticeable impact on cell wall development. In concordance with this hypothesis, *p4h5* mutant with deficient EXT *O*-arabinosylation showed an altered cell wall overall architecture in the root hair growing tip with drastically reduced growth (Velasquez et al., 2011; Velasquez et al., 2014). EXTs are relevant not only in root hair growth but also in cell plate formation in developing embryonic cells (Cannon et al., 2008), wall regeneration in tobacco protoplast (Cooper et al., 1994), in callus water hydration regulation (Jackson et al., 2001), and most

probably in many other cell types and developmental processes. In the present work we propose that the control of root hair tip growth by EXTs and EXT-related proteins in the cell walls may represent a more general mechanism to modulate cell elongation in other plant cell types such as pollen tubes, epidermal cells or trichomes. Recently, loss-of-function mutations in HPAT-encoding genes (*hpat1-hpat3*) as well as in SERGT1 (*sergt1*) have been reported to cause pleiotropic phenotypes confirming that *O*-glycosylation (Hyp-*O*-Arabinosylation and Ser-O-Galactosylation) in EXTs and related HRGPs is essential for both vegetative and reproductive development in *Arabidopsis* (Ogawa-Ohnishi et al., 2013; Saito et al., 2014). It is important to underline that *hpat1-hpat3* and *sergt1* mutants showed opposite phenotypes. Contrasting phenotypes such as larger roots versus shorter root hairs were reported for *sergt1* (Saito et al., 2014), and longer hypocotyls grown in the dark opposed to shorter pollen tubes (Ogawa-Ohnishi et al., 2013) and abnormal root hairs (this work) for the *hpat1-hpat3* mutants. Although we would expect that the EXT network would function in a similar way in any plant cell wall, the mode of cell expansion is very different in root hairs/pollen tubes (tip growth) in comparison to root cells/hypocotyls (anisotropic growth). While tip growth has a predominant single direction and the cell is isolated, in the anisotropic type there are two directions, being one predominant and each cell is contact to several other cells and the cell expansion is a highly coordinated process. Therefore, a deficient putative EXT network assembly would differentially affect expansion in each of these cell types. Besides, it is difficult to predict accurately how the PTMs (Post-Translational Modifications) in EXTs and other HRPGs would actually influence cell expansion in each particular cell type. In addition, cellulose and other polysaccharides interacting with each other in the expanding cells are also crucial to direct growth, and consequently, EXT-polysaccharide complexes would have to be considered as well. Further studies will aid to uncover the molecular mechanisms by which plant cells orchestrate the assembly of these complex EXT-polysaccharide networks during cell development.

LEGEND

Figure 1. Impact of deficient EXT *O*-glycosylation on root hair tip growth. A. *In silico* expression profiling of P4Hs and GTs associated with EXTs and related HRGPs using Genevestigator. Signal intensity values are arbitrary units. Only root tissues are shown. **B.** Co-expression analysis of P4H2 and P4H5 revealed the SERGT1 and HPAT3, as well as the already reported RRA3 and XEG113 proteins involved in post-translational modification of EXTs and related HRGPs. Co-expression values are based on *Pearson* correlation coefficients where r-value range from -1 for absolute negative correlation, 0 for no correlation and 1 for absolute positive correlation. **C.** Root hair phenotype of mutants in the *O*-glycosylation pathway (mean ± s.e.m., n= 200). 1A-3A= AraT mutants 1-3 arabinosyl units on each Hyp. **D.** Root hair phenotype in *hpat1-hpat3*, *rra3, xeg113-1* and *sergt1-1* mutants and Wt. Scale bar, 600 µm. **E-F.** Effects on root hair growth upon blocking of Hyp-*O*-arabinosylation of EXTs with P4H inhibitors (DP and EDHB) (mean ± s.e.m., n= 200). NT= non-treated. **F.** Root hair phenotype of untreated Wt, *sergt1-1*, and Wt and *sergt1-1* mutant treated with P4H inhibitors (DP and EDHB). Treated *sergt1-1* showed a drastic reduction of root hair growth when compared with untreated *sergt1-1*. **G-H.** Comparative effects on root hair growth in Wt, single mutants deficient in Hyp-*O*-arabinosylation (*p4h5* and *rra3*), a mutant deficient in Ser-*O*-Galactosylation (*sergt1-1*) and *p4h5 sergt1-1* and *rra3 sergt1-1* double mutants (mean ± s.e.m., n= 200). Single mutants are compared to Wt Col-0. Double mutants are compared to the corresponding single mutants. **I.** Time series of root hairs growth of Wt, *O*-glycosylation deficient mutant lines and P4H5 overexpressor line (35Spro::P4H5-GFP; pro=promoter). Asterisk indicates approximate time point of cessation of growth. **J.** EXT labeling in root hair cell walls with JIM20 antibody. Scale bar, 20 µm. (*) weak or (**) absence of labeling, and (♦) strong labeling. For Fig. 1C, 1E and 1G, P values of one-way analysis of variance (ANOVA) test, (**) $P < 0.01$, (***) $P < 0.001$ are shown.

Figure 2. Impact of deficient *O*-glycosylation on EXT proposed triple helix-like conformation. Structure and dynamics of Tyr-crosslinked, triple-helix organized EXT peptides. **A.** Schematics for the lateral alignment of EXT chains and Tyr-interchain-crosslink types. Only Tyr residues are depicted with their chemical structure. **B.** Center of mass distances between each EXT chain composing the non-glycosylated (blue) and Wt glycosylated (green) three helical structures, as a function of time: chain A to chain B (B1), chain A to chain C (B2) and chain B to chain C (B3). **C-E.** A representative structure of each simulated system is shown expanded 3 times in the x axis, as a preview of EXT and collagen physiological organization. In the structures, each of the three crosslinked chains are shown in decreasing shades of a same color, being chain A the darker and chain C the brighter. The peptides are presented in cartoon representation, and the Tyr crosslinks as red lines. The presented average energies represent the sum of the interaction between chain A to chain B, chain A to chain C and chain B to chain C.

REFERENCES

Cannon MC, Terneus K, Hall Q, Tan L, Wang Y, Wegenhart BL, Chen L, Lamport DT, Chen Y, Kieliszewski MJ (2008) Self-assembly of the plant cell wall requires an extensin scaffold. Proc Natl Acad Sci U S A **105:** 2226-2231

Cooper JB, Heuser JE, Varner JE (1994) 3, 4-Dehydroproline inhibits cell wall assembly and cell division in tobacco protoplasts. Plant physiology **104:** 747-752

Egelund J, Obel N, Ulvskov P, Geshi N, Pauly M, Bacic A, Petersen BL (2007) Molecular characterization of two Arabidopsis thaliana glycosyltransferase mutants, rra1 and rra2, which have a reduced residual arabinose content in a polymer tightly associated with the cellulosic wall residue. Plant Mol Biol **64:** 439-451

Gille S, Hansel U, Ziemann M, Pauly M (2009) Identification of plant cell wall mutants by means of a forward chemical genetic approach using hydrolases. Proc Natl Acad Sci U S A **106:** 14699-14704

Held MA, Tan L, Kamyab A, Hare M, Shpak E, Kieliszewski MJ (2004) Di-isodityrosine is the intermolecular cross-link of isodityrosine-rich extensin analogs cross-linked in vitro. Journal of Biological Chemistry **279:** 55474-55482

Ishiwata A, Kaeothip S, Takeda Y, Ito Y (2014) Synthesis of the Highly Glycosylated Hydrophilic Motif of Extensins. Angewandte Chemie **126:** 9970-9974

Jackson PA, Galinha CI, Pereira CS, Fortunato A, Soares NC, Amancio SB, Pinto Ricardo CP (2001) Rapid deposition of extensin during the elicitation of grapevine callus cultures is specifically catalyzed by a 40-kilodalton peroxidase. Plant Physiol **127:** 1065-1076

Matsubayashi Y (2010) [Glycopeptide hormones regulating plant growth and development]. Seikagaku **82:** 541-545

Nuñez A, Fishman ML, Fortis LL, Cooke PH, Hotchkiss Jr AT (2009) Identification of extensin protein associated with sugar beet pectin. Journal of agricultural and food chemistry **57:** 10951-10958

Ogawa-Ohnishi M, Matsushita W, Matsubayashi Y (2013) Identification of three hydroxyproline O-arabinosyltransferases in Arabidopsis thaliana. Nat Chem Biol **9:** 726-730

Ohyama K, Shinohara H, Ogawa-Ohnishi M, Matsubayashi Y (2009) A glycopeptide regulating stem cell fate in Arabidopsis thaliana. Nat Chem Biol **5:** 578-580

Owens NW, Stetefeld J, Lattova E, Schweizer F (2010) Contiguous O-galactosylation of 4(R)-hydroxy-l-proline residues forms very stable polyproline II helices. J Am Chem Soc **132:** 5036-5042

Ringli C (2010) The hydroxyproline-rich glycoprotein domain of the Arabidopsis LRX1 requires Tyr for function but not for insolubilization in the cell wall. Plant J **63:** 662-669

Saito F, Suyama A, Oka T, Yoko-o T, Matsuoka K, Jigami Y, Shimma Y (2014) Identification of novel peptidyl serine O-galactosyltransferase gene family in plants. Journal of Biological Chemistry **In press. doi. 10.1074/jbc.M114.553933**

Shinohara H, Matsubayashi Y (2013) Chemical Synthesis of Arabidopsis CLV3 Glycopeptide Reveals the Impact of Hydroxyproline Arabinosylation on Peptide Conformation and Activity. Plant and Cell Physiology **54:** 369-374

Shpak E, Barbar E, Leykam JF, Kieliszewski MJ (2001) Contiguous hydroxyproline residues direct hydroxyproline arabinosylation in Nicotiana tabacum. Journal of Biological Chemistry **276:** 11272-11278

Smallwood M, Beven A, Donovan N, Neill SJ, Peart J, Roberts K, Knox JP (1994) Localization of cell wall proteins in relation to the developmental anatomy of the carrot root apex. The Plant Journal **5:** 237-246

Valentin R, Cerclier C, Geneix N, Aguie-Beghin V, Gaillard C, Ralet MC, Cathala B (2010) Elaboration of extensin-pectin thin film model of primary plant cell wall. Langmuir **26:** 9891-9898

Velasquez SM, Ricardi MM, Dorosz JG, Fernandez PV, Nadra AD, Pol-Fachin L, Egelund J, Gille S, Harholt J, Ciancia M, Verli H, Pauly M, Bacic A, Olsen CE, Ulvskov P, Petersen BL, Somerville C, Iusem ND, Estevez JM (2011) O-Glycosylated Cell Wall Proteins Are Essential in Root Hair Growth. Science **332:** 1401-1403

Velasquez SM, Ricardi MM, Poulsen CP, Oikawa A, Dilokpimol A, Halim A, Mangano S, Denita Juarez SP, Marzol E, Salgado Salter JD, Dorosz JG, Borassi C, Moller SR, Buono R, Ohsawa Y, Matsuoka K, Otegui MS, Scheller HV, Geshi N, Petersen BL, Iusem ND, Estevez JM (2014) Complex Regulation of Prolyl-4-Hydroxylases Impacts Root Hair Expansion. Mol Plant http://dx.doi.org/10.1016/j.molp.2014.11.017.

ACKNOWLEDGEMENTS

We would like to thank J.P. Muschietti for critical reading of the manuscript. We thank ABRC (Ohio State University) for providing T-DNA lines seed lines. N.D.I., and J.M.E. are investigators of the National Research Council (CONICET) from Argentina. This work was supported by grants from ANPCyT (PICT2011-054 and PICT2013-003 to J.M.E and PICT 2011-967 to N.D.I.), CONICET (PIP0071 to J.M.E. and PIP0342 to N.D.I.), Mizutani Foundation for Glycoscience (Grant 130004 to J.M.E.), Fulbright-CONICET and Fulbright-Bunge & Born Fellowships (to J.M.E and S.M.V, respectively), CNPq, FAPERGS and CAPES to L.P-F. and H.V., and FACEPE (grant APQ-0398-1.06/13 to L.P-F.).

AUTHOR CONTRIBUTION

S.M.V. performed most of the experiments and analyzed the data. C.B., E.M., M.M.R., S.P.D.J., S.M., J.S.S, and J.G.D. analyzed and performed some of the experiments and analyzed the data. S.E.M. and J.P.K performed in situ antibody analysis of EXTs. J.R.D. analyzed root hair growth dynamics. L.P-F. and H.V. executed the molecular dynamics of EXT peptides. N.D.I. analyzed the data. J.M.E. designed research, analyzed the data, supervised the project, and wrote the paper. All authors commented on the results and the manuscript. This manuscript has not been published and is not under consideration for publication elsewhere. All the authors have read the manuscript and have approved this submission.

Competing financial interest

The authors declare no competing financial interests. Correspondence and requests for materials should be addressed to J.M.E. (Email: jestevez@fbmc.fcen.uba.ar).

Figure 1

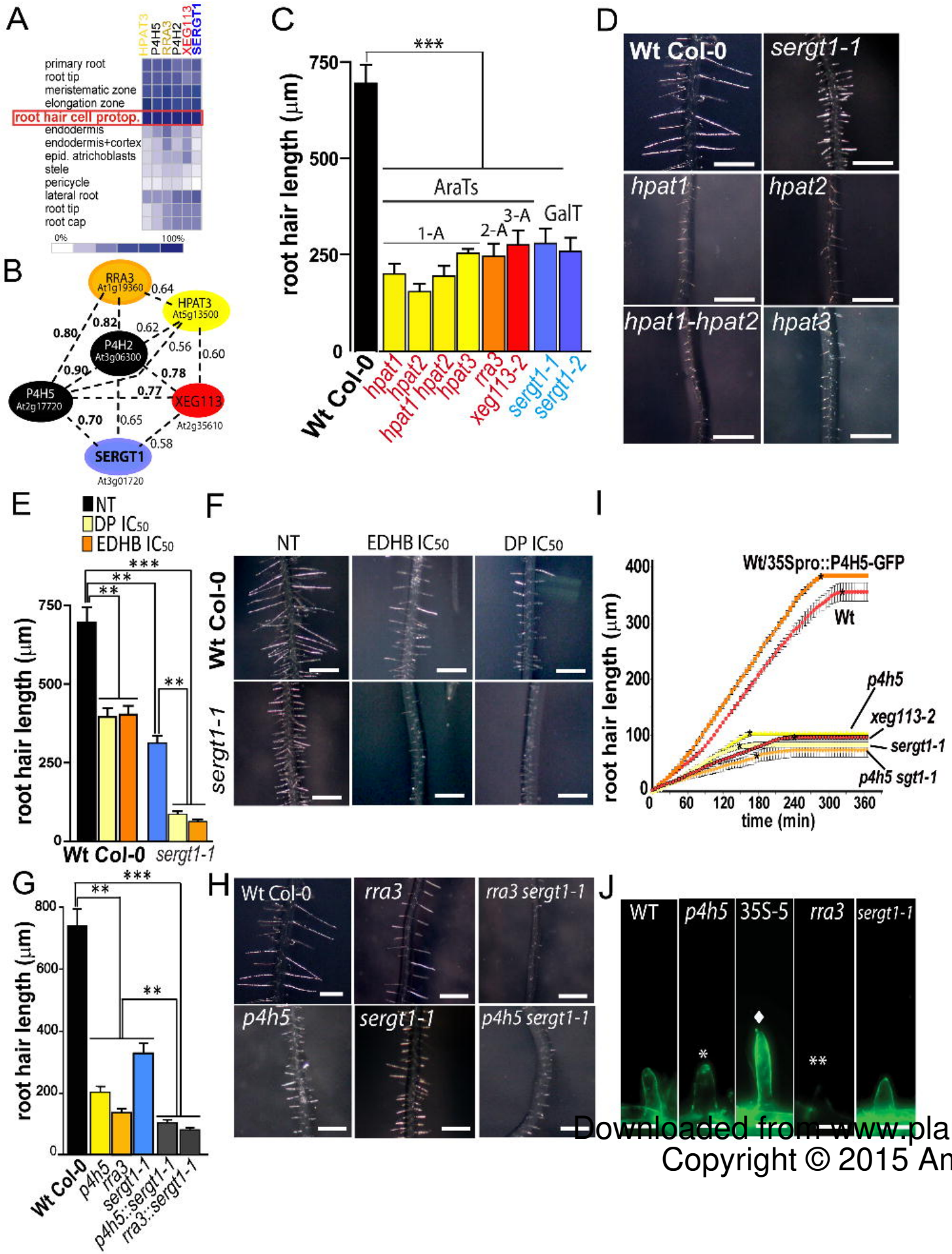

Figure 2

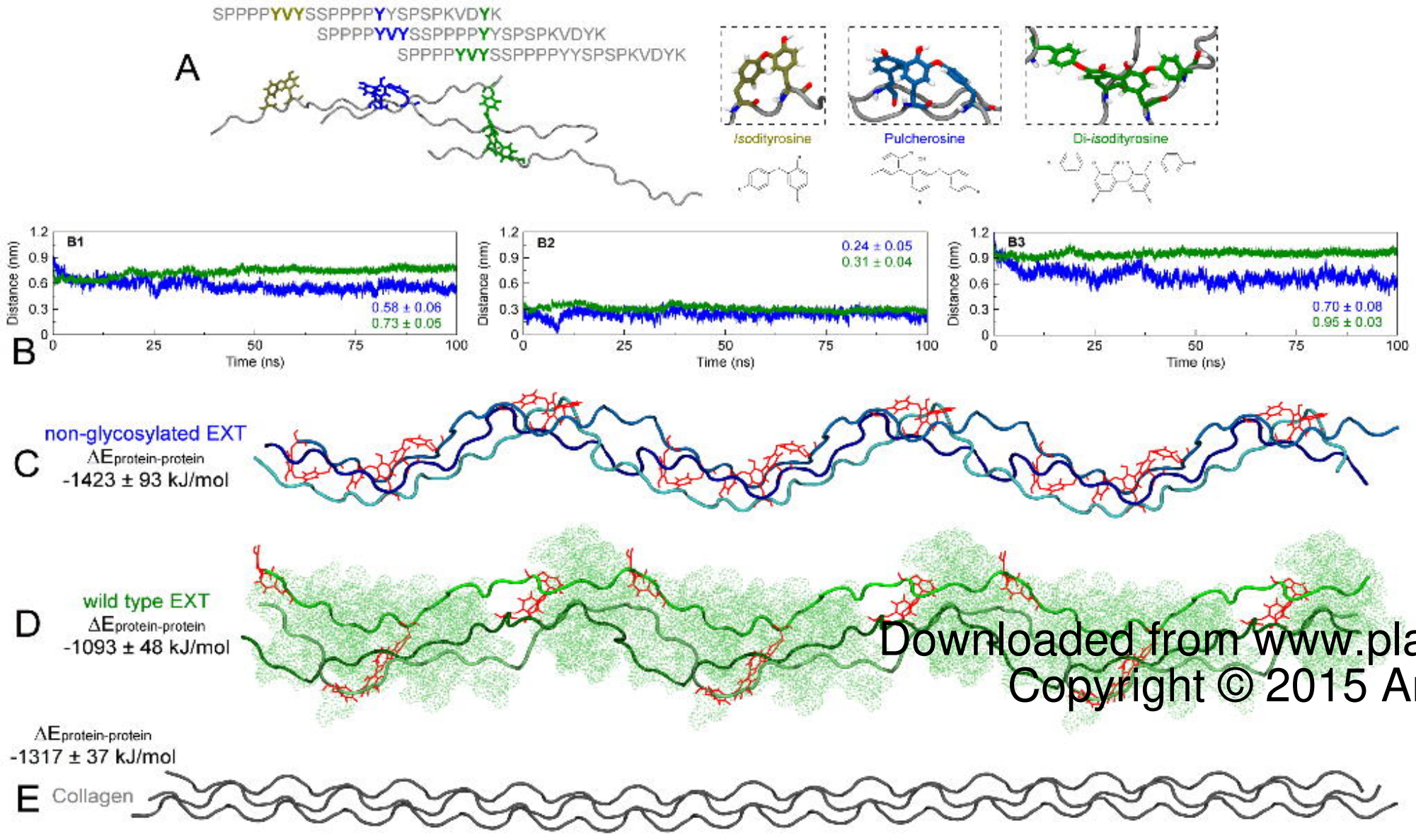

Scientific Correspondence

Supplementary Text

Low sugar is not always good: Impact of specific *O*-glycan defects on tip growth in *Arabidopsis*

Silvia M. Velasquez[1], Eliana Marzol[1], Cecilia Borassi[1], Laercio Pol-Fachin[2,3], Martiniano M. Ricardi[1], Silvina Mangano[1], Silvina Paola Denita Juarez[1], Juan D. Salgado Salter[1], Javier Gloazzo Dorosz[1], , Susan E. Marcus[4], J. Paul Knox[4], Jose R. Dinneny[5], Norberto D. Iusem[1,6], Hugo Verli[3] & José M. Estevez[1,†]

[1]Instituto de Fisiología, Biología Molecular y Neurociencias (IFIBYNE-CONICET), Facultad de Ciencias Exactas y Naturales, Universidad de Buenos Aires C1428EGA, Argentina.
[2]Departamento de Química Fundamental, Universidade Federal de Pernambuco, Brasil.
[3]Centro de Biotecnologia, Universidade Federal do Rio Grande do Sul, Brasil.
[4]Centre for Plant Sciences, Faculty of Biological Sciences, University of Leeds, Leeds LS2 9JT, UK.
[5]Carnegie Institution for Science, Department of Plant Biology, Stanford, California 94305.
[6]Departamento de Fisiología, Biología Molecular y Celular. Laboratorio de Fisiología y Biología Molecular (LFBM), Facultad de Ciencias Exactas y Naturales, Universidad de Buenos Aires, Buenos Aires C1428EGA, Argentina.

[†] Correspondence should be addressed. Email: jestevez@fbmc.fcen.uba.ar

EXPERIMENTAL PROCEDURES

Plant Materials. *Arabidopsis thaliana* Columbia-0 (Col-0) was used as the wild type (Wt) genotype. Seedlings were germinated on half-strength MS agar plates in a Percival incubator at 22°C in a growth room with 16h light/8h dark cycles for 7-10 days. Plants were transferred to soil for growth under the same conditions as previously described.

T-DNA mutant analysis. For identification of T-DNA knockout lines, genomic DNA was extracted from rosette leaves (Weigel and Glazebrook, 2002). Confirmation by PCR of a single and multiple T-DNA insertions in the target genes SERGT1 (*sergt1-1* SALK_054682 and *sergt1-2* SALK_059879), were performed using an insertion-specific LBb1 (for SALK lines) or Lb3 (for SAIL lines) primer in addition to one gene-specific primer. We isolated homozygous (for all the genes mentioned above). Homozygous *hpat1-1*, *hpat2-1*, and *hpat3-1* (Ogawa-Ohnishi et al., 2013), *xeg113-2* (Gille et al., 2009), *rra3* (GABI_233B05) (Velasquez et al., 2011) and *p4h5* T-DNA mutants (Velasquez et al., 2011) were isolated previously. Double mutants were generated by manual crosses of the corresponding single mutants. The primers used for *sergt1-1* SALK_054682 were: forward 5' GCAGACAAAGAACACTACGGG 3' and reverse 5' CATGAGAGAGAAAGTGGTCCG 3'. For *sergt1-2* SALK_059879, primers were: forward 5' GTGAGCTGTATCTTGGCGAAC 3' and reverse 5' AATCATCCTCCATGCATTGAC 3'. For *p4h5* SALK_152869, primers were: forward 5' CATTTTGAGAGCTCGTTCCAC 3' and reverse 5' TCACAATTTCTTGGTAATTTCGTG 3'. For *rra3* GABI_233B05, primers were: forward 5' GATTCAATATCACAGCCTCGC 3', reverse 5' AACCATGTCATACCTGCAAGC 3'. Primers for *hpat1,2,3* mutants are described elsewhere (Ogawa-Ohnishi et al., 2013).

Root hair phenotypic analysis (shown in **Fig.1 C,E,G**). For quantitative analysis of root hair phenotypes, 200 fully elongated root hairs from the whole root were measured (n roots= 20-30) from seedlings grown on vertical plates on agar 1% with no Murashige and Skoog addition for 7 days under continuous light. Values are reported as the mean ±SD using the Image J software. For measurements of root hair inhibition, P4H inhibitors ethyl-3,4-dihydrohydroxybenzoate (EDHB) (Barnett, 1970) and α,α-dipyridyl (DP)(Majamaa et al., 1986) were added to half-strength MS medium (Velasquez et al., 2011). Fully elongated root hairs (n= 150-200; n roots= 20-30) were analyzed at each P4H inhibitors' concentration. Twenty seedlings of each genotype were measured.

Live imaging of root hair growth and Data Analysis (shown in **Fig. 1I**). Seven-day old seedlings, grown on 0.5% Murashige and Skoog medium 0.7% GelRight under 18hs/6hs light/dark cycles, were imaged for a length of time of 24 hours with images taken every 5 minutes using a macroscopic imaging system described in (Duan et al., 2013). Images were processed by generating a stack of images with ImageJ software (Abramoff et al., 2004), then an algorithm described in (Geng et al., 2013) was used to enhance the contrast of edges, a 200 percent digital zoom was used to amplify selected areas were we could observe root hairs from the

moment of their initiation up to the moment when they stopped growing. The GR was calculated by dividing the total root hair length by the total time of growth. The total time growth was calculated by summing up all of the time points for each root hair (from its initiation to its completion). At least 10 root hairs were analyzed for each mutant.

Root hair EXT immunolabeling. The root surfaces of intact *A. thaliana* seedlings were immunolabeled with monoclonal antibody JIM20 (Smallwood et al., 1994) according to the indirect immunolabeling technique used for intact seedlings. Seedlings were fixed O/N in 4% paraformaldehyde in 50 mM piperazine-N,N-bis(2-ethane-sulphonic acid) (PIPES), 5 mM MgSO4, and 5 mM ethylene glycol tetra-acetic acid (EGTA). Prior to immunolabeling, intact seedlings were incubated in 5% (w/v) milk protein in phosphate-buffered saline (MP/PBS) for 1 h; then incubated in primary antibody JIM20 diluted fivefold in MP⁄PBS for 1.5 h; washed for 3 x for 5 min in PBS; incubated with anti-rat immunoglobulin-G linked to fluorescein isothiocyanate (FITC; Sigma) diluted 100-fold in MP/PBS for 1 h in darkness. After a final washing seedlings were mounted in Citifluor antifade (Agar) and observed on an Olympus BX61 microscope equipped with a Hamamatsu ORCA285 camera and Volocity software (PerkinElmer, Massachusetts, USA).

Co-expression analysis network. Co-expression networks for P4H2, P4H5, RRA3, XEG113 and SERGT1 (cluster 172) were identified from AraNet (http://aranet.mpimp-golm.mpg.de/aranet) and trimmed to facilitate readability. Each co-expression of interest was confirmed independently using the expression angler tool from Botany Array Resource BAR (http://bar.utoronto.ca/ntools/cgi-bin/ntools_expression_angler.cgi) and ATTED-II (http://atted.jp). Only those genes that are connected with genes of interest are included. Co-expression values are based on *Pearson* correlation coefficients where r-value ranges from -1 for absolute negative correlation, 0 for no correlation and 1 for absolute positive correlation.

Molecular Dynamics (MD) simulations of EXT repeat sequence. Carbohydrates and peptides were described under GROMOS96 43A1 force field parameters and GROMACS simulation suite, version 4.0.5 (Hess et al., 2008). The glycan chains and carbohydrate-amino acid connections were constructed based on the most prevalent geometries obtained from solution MD simulations of their respective disaccharides (Pol-Fachin and Verli, 2012). The sequence SPPPPYVYSSPPPPYYSPSPKVYYK was built as a linear peptide, presenting ϕ/ψ backbone torsion angles compatible with type-II polyproline helixes (-75/145 degrees). In order to generate the glycosylated peptides, 4-*trans* hydroxyl groups were added to prolines in SPPPP moieties. Subsequently, *O*-glycosylation sites were filled with their proposed glycan chains, thus generating the initial coordinates for three glycopeptide MD simulations: only arabinosylated EXT, only galactosylated EXT and fully glycosylated EXT (Wt Col-0). In the case of EXT crosslinked sequences, the starting structure for MD simulations was generated by molecular replacement of the non-glycosylated SPPPPYVYSSPPPPYYSPSPKVYYK most prevalent peptide conformation with each chain in collagen three-helix structure in PDB ID 1K6F (Berisio et al., 2002).

Additionally, topologies for the crosslinked Tyr amino acid residues were compiled based on atomic charges, bonded and non-bonded parameters previously present within GROMOS96 43A1 force field. Such structures were then solvated in rectangular boxes using periodic boundary conditions, in which a covalent peptide bond was defined between the Ser and Lys amino acid residues at the box edge on the z-axis of SPPPPYVYSSPPPPYYSPSPKVYYK simulations, thus treating such polypeptide chains as “infinite” polymers. The employed MD protocol was based on a previous study (Velasquez et al., 2011), in which such simulations were extended to 100 ns.

LEGENDS TO FIGURES

Figure S1. A Post-translational modification steps of EXT and EXT-related proteins. Only the repetitive sequence Ser-(Pro)4 is shown. P4Hs converts peptidyl-Pro into Hyp. Hyp is then glycosylated by the sequential addition of arabinosyl units by arabinosyltransferases HPAT1-3, RRA3 and XEG113. In addition, Ser is mono-*O*-galactosylated by SERGT1. **B.** Arabinosylation of small peptides with up to three arabinose units. HPAT3 arabinosylates the small secreted peptide CLAVATA3. It is proposed that RRA3 and XEG113 would add the second and third arabinose unit.

Figure S2. Growth parameters and root hair length of *O*-glycan deficient mutants and 35S-P4H5 OX. **A.** Growth, **B** final growth time and **C** root hair length of Wt, *O*-glycosylation deficient mutant lines (*p4h5*, *sergt1*, *p4h5 sergt1*, *xeg113*) and P4H5 overexpressor line. P values of one-way analysis of variance (ANOVA) test, (*) $P < 0.01$, (***) $P < 0.001$. NS= not significant.

Figure S3. *O*-Glycosylation effect on EXT conformation. **A.** Representative frames from non-hydroxylated (black), *O*-galactosylated (red), *O*-arabinosylated (green) and Wt Col-0 glycosylation state (blue) of EXT minimal peptide in MD simulations, obtained as the most prevalent group from a clustering analysis on the entire trajectory with a 0.8 nm cutoff. In the structures, the peptide is shown as cartoon, Tyr residues are presented as sticks and *O*-linked glycan chains as dots. **B.** Distance between Tyr6:$C_\xi 2$ and Tyr8:OH during molecular dynamics simulations of SPPPP**Y**V**Y**SSPPPPYYSPSPKVYYK peptides.

Table S1. Biological properties of the enzymes involved in the posttranslational modifications of HRGPs.

Gene (AGI)/ CAZy	*Mutant*	*In vitro* activity	Subcellular localization	Tissue localization	Enzyme activity/ mutant phenotype	Reference
Prolyl 4-Hydroxylases (P4Hs)						
P4H2 (AT3G06300)	*p4h2-1; p4h2-2*	Yes	ER, Golgi	Root, Root Hairs	ND/ Short root hairs.	(Velasquez et al., 2011) (Tiainen et al., 2005)
P4H5 (AT2G17720)	*p4h5*	Yes	ER, Golgi	Root, Root Hairs	EXT proline-peptidyl hydroxylation / Short root hairs.	(Velasquez et al., 2011) (Velasquez et al., 2014)
P4H13 (AT2G23096)	*p4h13*	-	ER, Golgi	Root, Root Hairs	ND /Short root hairs.	(Velasquez et al., 2011)
Arabynosyltranferases (AraTs)			-	-		
AtHPAT1 (AT5G25265) GT8 AtHPAT2 (AT2G25260) GT8 AtHPAT3 (AT5G13500) GT8	*hpat1-1* *hpat2-1* *hpat3-1*	Yes Yes Yes	Golgi	Root Hairs	Hyp-O-arabinosyltransferase / impaired pollen tubes growth enhanced hypocotyl elongation, and early flowering. Short root hairs	(Ogawa-Ohnishi et al., 2013) This study
AtRRA1 (At1g75120) GT77 AtRRA2 (At1g75110) GT77	*rra1* *rra2*	ND ND	Golgi	-	ND/ Short root hairs. Reduced levels of arabinose in the mutant	(Petersen et al., 2011) (Egelund et al., 2007)
AtRRA3 (At1g19360) GT77	*rra3*	ND	Golgi	Root Hairs	ND/ Short root hairs. Reduced levels of arabinose in EXTs present in the mutant.	(Velasquez et al., 2011)
AtXEG113 (At2g35610) GT47	*xeg113-2*	ND	Golgi	Root Hairs	ND/ Short root hairs. Reduced levels of arabinose in the mutant	(Gille et al., 2009) (Velasquez et al., 2011)
Galactosyltranferase (GalT)						
AtSERGT1 (At3g01720) GT96	*sergt1-1; sergt1-2*	Yes	Unknown	Root, Root Hairs	Serine galactosyltransferase activity/Short root hairs. Reduced levels of galactose in the mutant	(Saito et al., 2014) This study

ND= not detected.

References

Abramoff MD, Magalhaes PJ, Ram SJ (2004) Image processing with ImageJ. Biophotonics international **11:** 36-43

Barnett NM (1970) Dipyridyl-induced Cell Elongation and Inhibition of Cell Wall Hydroxyproline Biosynthesis. Plant Physiol **45:** 188-191

Berisio R, Vitagliano L, Mazzarella L, Zagari A (2002) Crystal structure of the collagen triple helix model [(Pro-Pro-Gly) 10] 3. Protein Science **11:** 262-270

Duan L, Dietrich D, Ng CH, Chan PMY, Bhalerao R, Bennett MJ, Dinneny JR (2013) Endodermal ABA signaling promotes lateral root quiescence during salt stress in Arabidopsis seedlings. The Plant Cell Online **25:** 324-341

Egelund J, Obel N, Ulvskov P, Geshi N, Pauly M, Bacic A, Petersen B (2007) Molecular characterization of two *Arabidopsis thaliana* glycosyltransferase mutants, *rra1* and *rra2*, which have a reduced residual arabinose content in a polymer tightly associated with the cellulosic wall residue. Plant Mol Biol **64:** 439-451

Geng Y, Wu R, Wee CW, Xie F, Wei X, Chan PMY, Tham C, Duan L, Dinneny JR (2013) A spatio-temporal understanding of growth regulation during the salt stress response in Arabidopsis. The Plant Cell Online **25:** 2132-2154

Gille S, Hansel U, Ziemann M, Pauly M (2009) Identification of plant cell wall mutants by means of a forward chemical genetic approach using hydrolases. Proc Natl Acad Sci U S A **106:** 14699-14704

Hess B, Kutzner C, Van Der Spoel D, Lindahl E (2008) GROMACS 4: Algorithms for highly efficient, load-balanced, and scalable molecular simulation. Journal of chemical theory and computation **4:** 435-447

Majamaa K, Gunzler V, Hanauske-Abel HM, Myllyla R, Kivirikko KI (1986) Partial identity of the 2-oxoglutarate and ascorbate binding sites of prolyl 4-hydroxylase. J Biol Chem **261:** 7819-7823

Ogawa-Ohnishi M, Matsushita W, Matsubayashi Y (2013) Identification of three hydroxyproline O-arabinosyltransferases in Arabidopsis thaliana. Nat Chem Biol **9:** 726-730

Petersen BL, Faber K, Ulvskov P, Ulvskov P (2011) Glycosyltransferases of the GT77 family. Annual Plant Reviews: Plant Polysaccharides, Biosynthesis, and Bioengineering**:** 305-320

Pol-Fachin L, Verli H (2012) Structural glycobiology of the major allergen of Artemisia vulgaris pollen, Art v 1: O-glycosylation influence on the protein dynamics and allergenicity. Glycobiology **22:** 817-825

Saito F, Suyama A, Oka T, T Y-O, Matsuoka K, Jigami Y, Shimma Y (2014) Identification of novel peptidyl serine *O*-galactosyltransferase gene family in plants. J Biol Chem **DOI. 10.1074/jbc.M114.553933**

Smallwood M, Beven A, Donovan N, Neill SJ, Peart J, Roberts K, Knox JP (1994) Localization of cell wall proteins in relation to the developmental anatomy of the carrot root apex. The Plant Journal **5:** 237-246

Tiainen P, Myllyharju J, Koivunen P (2005) Characterization of a second Arabidopsis thaliana prolyl 4-hydroxylase with distinct substrate specificity. J Biol Chem **280:** 1142-1148

Velasquez S, Ricardi M, Dorosz J, Fernandez P, Nadra A, Pol-Fachin L, Egelund J, Gille S, Harholt J, Ciancia M, Verli H, Pauly M, Bacic A, Olsen C, Ulvskov P, Petersen B, Somerville C, Iusem N, Estevez J (2011) *O*-glycosylated cell wall proteins are essential in root hair growth. Science **332:** 1401-1403

Velasquez SM, Ricardi MM, Poulsen CP, Oikawa A, Dilokpimol A, Halim A, Mangano S, Denita Juarez SP, Marzol E, Salgado Salter JD, Dorosz JG, Borassi C, Moller SR, Buono R, Ohsawa Y, Matsuoka K, Otegui MS, Scheller HV, Geshi N, Petersen BL, Iusem ND, Estevez JM (2014) Complex Regulation of Prolyl-4-Hydroxylases Impacts Root Hair Expansion. Mol Plant

Weigel D, Glazebrook J (2002) Arabidopsis: A Laboratory Manual. Cold Spring Harbor Laboratory Press

Figure S1

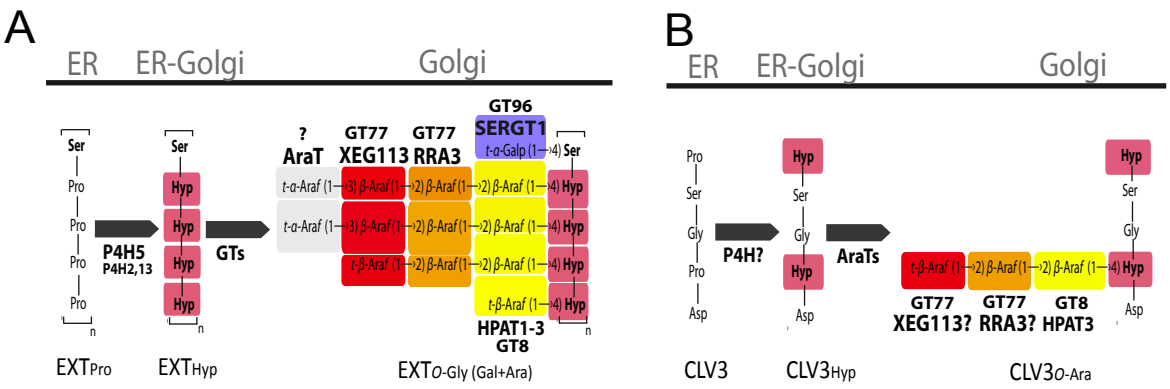

Figure S1. A Post-translational modification steps of EXT and EXT-related proteins. Only the repetitive sequence Ser-(Pro)4 is shown. P4Hs converts peptidyl-Pro into Hyp. Hyp is then glycosylated by the sequential addition of arabinosyl units by arabinosyltransferases HPAT1-3, RRA3 and XEG113. In addition, Ser is mono-*O*-galactosylated by SERGT1. **B.** Arabinosylation of small peptides with up to three arabinose units. HPAT3 arabinosylates the small secreted peptide CLAVATA3. It is proposed that RRA3 and XEG113 would add the second and third arabinose unit.

Figure S2

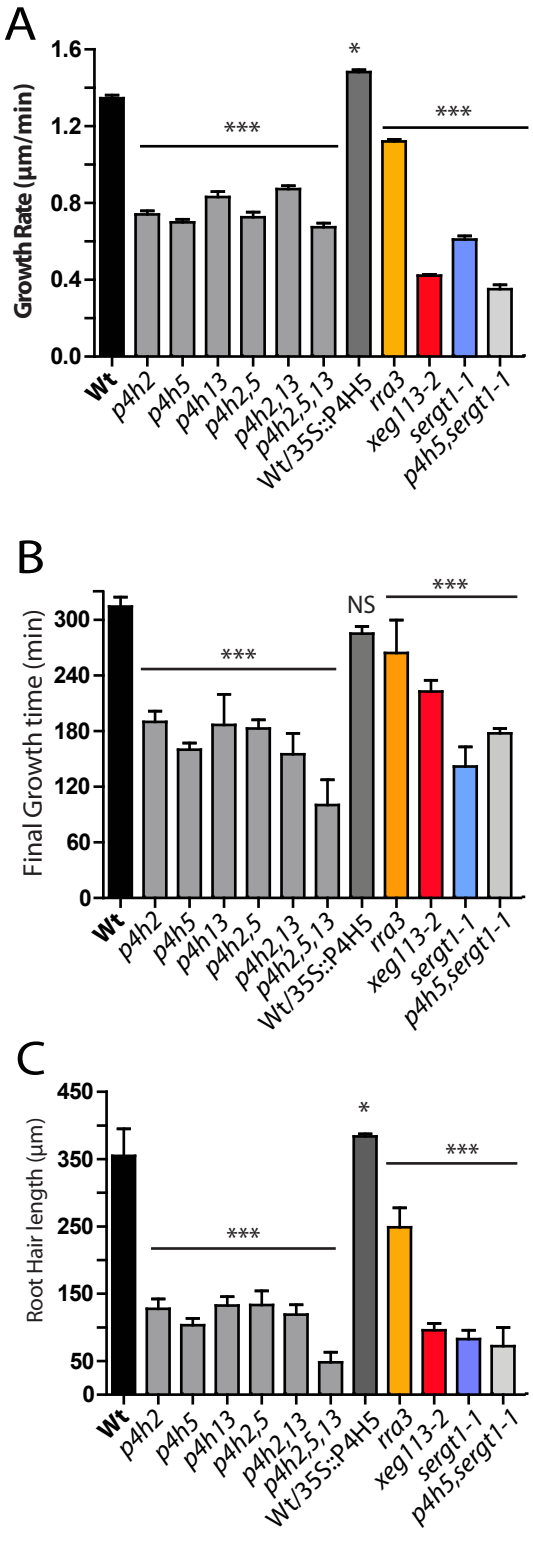

Figure S2. Growth parameters and root hair length of *O*-glycan deficient mutants and 35S-P4H5 OX. **A.** Growth, **B** final growth time and **C** root hair length of Wt, *O*-glycosylation deficient mutant lines (*p4h5*, *sergt1*, *p4h5 sergt1*, *xeg113*) and P4H5 overexpressor line. P values of one-way analysis of variance (ANOVA) test, (*) $P < 0.01$, (***) $P < 0.001$. NS= not significant.

Figure S3

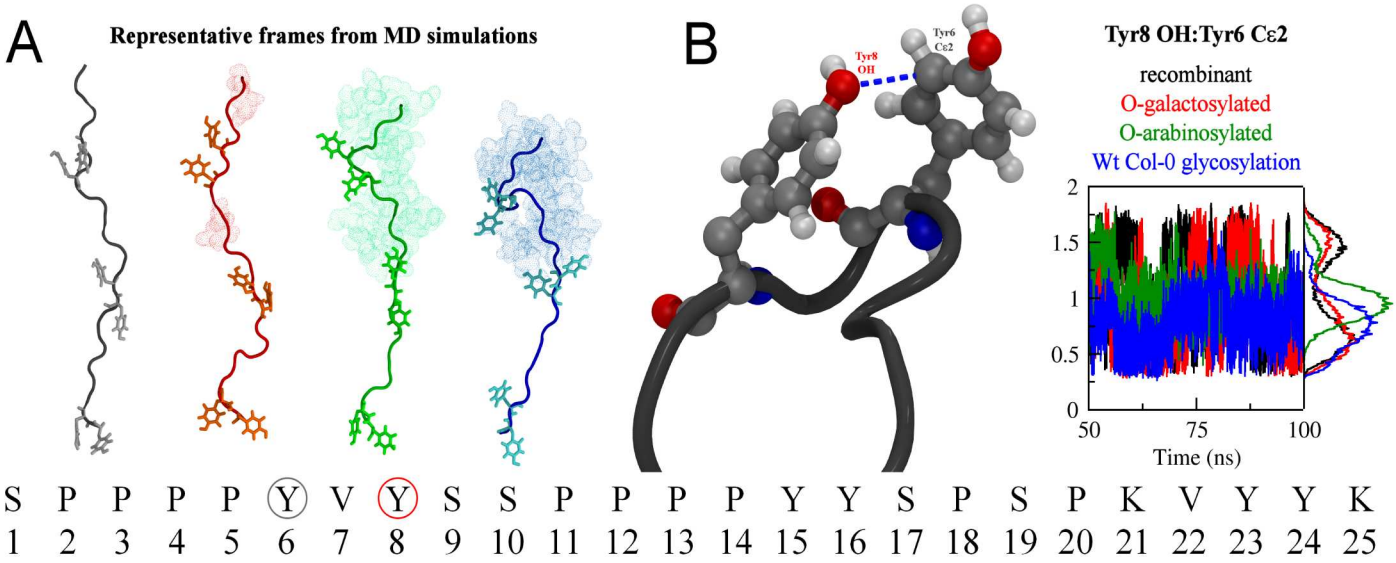

Figure S3. *O*-Glycosylation effect on EXT conformation. **A.** Representative frames from non-hydroxylated (black), *O*-galactosylated (red), *O*-arabinosylated (green) and Wt Col-0 glycosylation state (blue) of EXT minimal peptide in MD simulations, obtained as the most prevalent group from a clustering analysis on the entire trajectory with a 0.8 nm cutoff. In the structures, the peptide is shown as cartoon, Tyr residues are presented as sticks and *O*-linked glycan chains as dots. **B.** Distance between Tyr6:C$_\xi$2 and Tyr8:OH during molecular dynamics simulations of SPPPP**Y**V**Y**SSPPPPYYSPSPKVYYK peptides.